Bending Angle Effect of the Cross-Section Ratio for a Soft Pneumatic Actuator

Jutamanee Auysakul, Nitipan Vittayaphadung, Sarawut Gonsrang, and Pruittikorn Smithmaitrie
Department of Mechanical Engineering, Faculty of Engineering,
Prince of Songkla University, Hat Yai, Songkhla 90112, Thailand
Email: jutamanee.a@psu.ac.th, nitipan.v@psu.ac.th, gsarawut@eng.psu.ac.th and pruittikorn.s@psu.ac.th

***Abstract*— A soft pneumatic actuator is a soft robotics part that significantly increases ability of a robotic arm to grasp an object in the automatic production line. To grip an object of various sizes and shapes, the bending angle of the actuator is a parameter that affects the grasping area and positioning of a robotic arm while applying air pressure. In this study, the actuator models with small and large cross-section ratios are compared by simulation using the finite element method. The simulation results show that increasing of the model cross-section ratio provides the wider bending angle than the reduced cross-section ratio model or the basic configuration model at the same input pressure. The proposed model still maintains the air surface area inside the actuator. Furthermore, it was found that the reduced cross-section ratio model has the most significant influence on the bending angle than the other models. Thus, the model comparison in term of the cross-section ratio is helpful to design the most effective gripper.**

***Index Terms*—soft pneumatic actuator, soft robotic gripper, mathematical modeling, soft robotics**

I. Introduction

Soft robot research has become increasingly popular in the robotic field. One of the main reasons is that soft robots can perform unique actions such as grasping objects of various sizes and shapes safely, deliver high power and safely interact with human operators. Additionally, the technology is usually lightweight and cheap. In contrast, conventional robots have stiff designs. [1]. Therefore, soft actuators, which can execute fast, precise and strong operations, have been extensively used in automation, locomotion, and rehabilitation. Accordingly, soft actuators have evolved to behave like natural muscles [2].

Soft actuators that operate with air pressure are called soft pneumatic actuators (SPAs). Some use shape-memory alloy [3], [4] or hydraulics [5] to drive the peripheral components. SPAs are applied via a pneumatic network to generate bending action and movement that are inspired by animals; for example, a soft gripper like a human finger can play a digital keyboard [6]. A multi-gait quadruped is inspired by an octopus and can produce complex motions [7]. The simple structure of a SPA combines a hollow shape with a thin membrane made of silicone. This special polymer is flexible enough to be stretched while air pressure is being applied [8]-[11]. Polyether ketones and PVC coating films are used when the actuators require complex structures like zigzag origami [12], which is currently a trend in the robotic field. Furthermore, several fabrication techniques are used to produce SPAs using two-step molding technique [13], silicone 3D printer [14] or dissolvable core technique.

The chamber geometry is a significant design parameter which affects the bending performance. Hu *et al*. [15] introduced an optimization approach that selected optimal parameters like the bottom layer thickness, gap size between adjacent chambers, wall thickness, and chamber cross section. The work also illustrated how the finite element method (FEM) is useful to optimize geometric variables and validated the findings via experimental methods. This work investigates cross-section ratios and parameters that influence bending performance. The optimized parameter in this study is the ratio between the size of the first and last chamber. The ratio is optimized by finite element analysis.

This paper is organized in the following way. In Section II, the basic SPA configuration and the SPA designs are introduced and compared. Section III describes how FEM is used to simulate the models by comparing in terms of bending analysis. The simulation results of each model are shown in Section IV. Finally, Section V concludes this work.

II. SPA Design and Configuration

A. Basic Configuration of a SPA

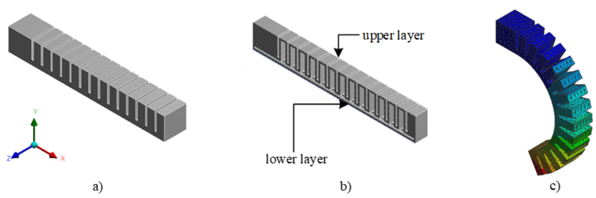

Figure 1. The basic configuration of a SPA. (a) basic model; (b) cross-sectional view; and (c) bending effect.

The basic configuration of a SPA as shown in Fig. 1(a) composes of an upper layer and base layer. The configuration reveals of air chambers and air channels as shown in Fig. 1(b). The SPA actuation depends on

Manuscript received April 10, 2019; revised December 4, 2019.

doi: 10.18178/ijmerr.9.3.366-370

applied pneumatic pressure to the air chambers. The SPA is made of a hyper-elastic material. Thus, the chamber walls are flexible enough to stretch during operation.

Fig. 1(c) shows the SPA deformation caused by the pressurized air in the chambers, which generates stresses on the walls in the x- and y-axes. However, if the stress in the x-axis is greater than the stress in the y-axis, then the chamber is stretched horizontally according to the SPA bending requirements. This actuation effect can be used to enact a grasping motion which can pick up and move objects of various sizes and shapes.

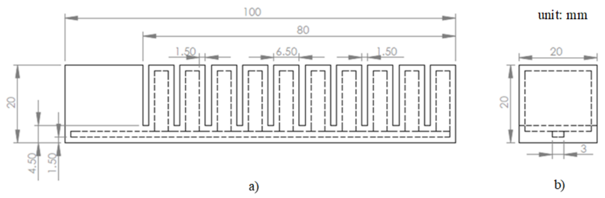

Figure 2. Dimension of the basic SPA design (a) front view and (b) right view.

The basic SPA design includes 10 air chambers for a model with the length of 100 mm and the cross-sectional area of 20x20 mm^2, as shown in Fig. 2. It can be compressed by 20 mm (i.e., to the length of 80 mm) so that the actuator can grasp objects like a human finger. The chambers gap size is 1.5 mm to enable the stretching action between the chambers. The chamber has the width and wall thickness of 6.5 mm and 1.5 mm, respectively.

Consequently, the SPA lower layer has the thickness of 4.5 mm and 3x1.5 mm^2 air channel bored through the last chamber equalizing the air pressure. The dimensions of the wall thickness, gap and the bottom layer have been optimized as in Hu *et al*. [15]. Hence, this basic SPA configuration is used to compare the bending efficiency with the other proposed.

B. Comparative Design of the SPA

In this work, there are 6 different SPA designs with cross-sectional areas as shown in Fig. 3. Those designs are separated by angle, obliquely up and down, as illustrated in Models 1-3 and Models 4-6, respectively. The surface area, gap and thickness of the chamber are identical in dimension as of the basic SPA configuration. However, to compare the bending performance among the models, the surface area of the air chamber has to be the same as the basic SPA model surface area (8,217 mm^2). Therefore, the height of the model is varied in terms of the surface area, with the deviation of the surface area less than 5% compared with the basic model, as shown in Table I.

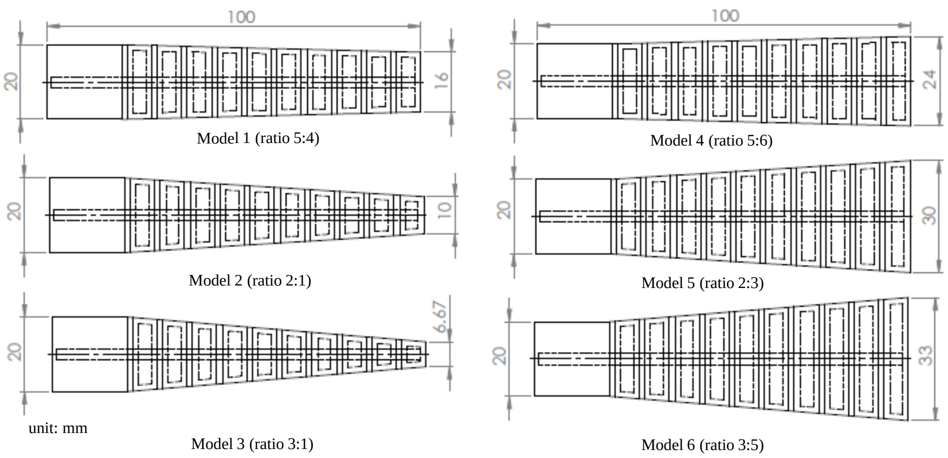

Figure 3. The proposed SPA model variation.

TABLE I. SURFACE AREA OF AIR CHAMBERS WITH DIFFERENT HEIGHT

SPA design	Surface area (mm^2)	Area deviation (%)	Height (mm)
Model 1	8222.7	-0.07	22.1
Model 2	8227.1	-0.12	26.3
Model 3	8218.9	-0.02	29.4
Model 4	8229.4	-0.15	18.3
Model 5	8211.8	0.06	16.2
Model 6	8242.3	-0.31	15.4

III. FEM ANALYSIS METHOD

FEM is a powerful tool that is extensively used to optimize and predict effects of innovative designs before manufacturing the product. In this work, the static structure analysis was conducted to validate the model parameters, which focuses on the deformation characteristics of the SPA models under air pressurized loading. The boundary conditions include a fixed displacement on the left side floor and wall. The air pressure is applied to the inside of each chamber as shown in Fig. 4.

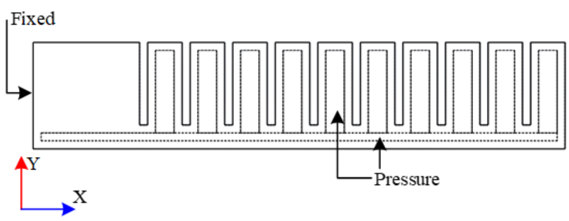

Figure 4. Boundary conditions of the SPA model.

The pneumatic pressure varies from 1 kPa to 20 kPa to investigate the actuator deformation. The finite element model is fine-meshed due to the large deformation effect of a nonlinear material in the element. Additionally, the applied pressure was initially set over 500 substeps. These fine steps give smooth transition of the computational results. Then, the FEM results are used to optimize the cross-section ratio of the models by comparison the and later being validate by the experimental testing.

A. Material Selection

Silicone rubber is selected for modelling because it supports soft robot behavior. That is the silicone model facilitates high bending angle while applying the air pressure. This material has many advantages in terms of its flexibility, inexpensive cost and malleability. In this research, normal grade silicon rubber (with shore A 25-45) is used because it is generally available in the market. The silicone rubber properties are shown in Table II.

Silicon rubber is a hyper-elastic material, so a third-order Mooney-Rivlin property is needed to define the stress-strain property effectively. This property was tested using a tensile strength tester under the ASTM D412 test method.

TABLE II. THE MATERIAL PROPERTIES OF THE SILICON RUBBER.

Properties	Value
Hardness Shore A	30
Poisson ration	0.49
Elongation at break	460%
Mix ratio	1:1
Density	1.208 g/cm^3

B. Bending Angle Analysis

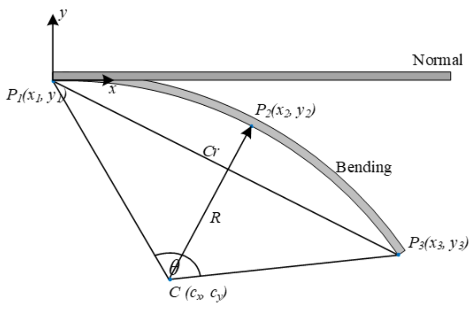

Figure 5. Bending angle reference and parameters.

As the pressurized air flows into the SPA chambers, the actuator is stretched with various bending angles depending on air pressure. To define the bending performance of the SPA, the bending angle θ, as shown in Fig. 5, is calculated by using the measured point P_2 and P_3 with the reference point P_1. The center of the arc C is determined as follows:

$$\begin{bmatrix} 2(x_2 - x_1) & 2(y_2 - y_1) \\ 2(x_3 - x_1) & 2(y_3 - y_1) \end{bmatrix} \begin{bmatrix} c_x \\ c_y \end{bmatrix} = \begin{bmatrix} x_2^2 + y_2^2 - x_1^2 - y_1^2 \\ x_3^2 + y_3^2 - x_1^2 - y_1^2 \end{bmatrix} \quad (1)$$

where the point P_2 and P_3 are in the end and middle position of an actuator, respectively. The center of the arc can be used to calculate the radius R as

$$R = \sqrt{(x_1 - c_x)^2 + (y_1 - c_y)^2} \quad (2)$$

The circular chord Cr is defined by

$$Cr = \sqrt{(x_1 - x_3)^2 + (y_1 - y_3)^2} \quad (3)$$

Thus, the bending angle can be expressed as

$$\theta = 2\sin^{-1}\left(\frac{Cr}{2R}\right) \quad (4)$$

The bending angle is helpful to design the SPA model that matches the grasping action requirement in the soft robotic gripper.

IV. FEM RESULTS OF THE COMPARATIVE MODELS

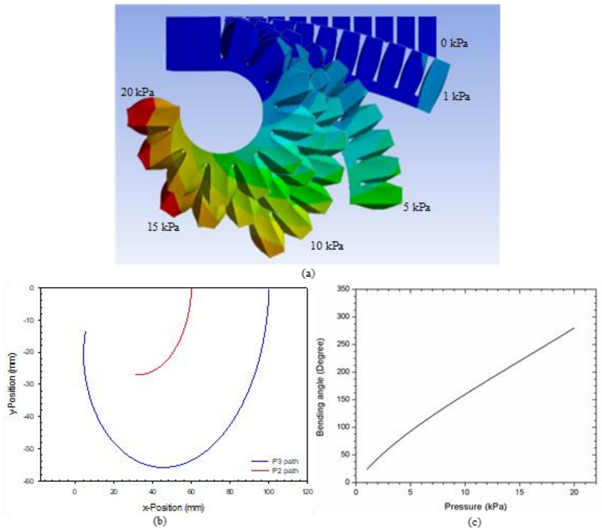

Figure 6. Deformation of the basic SPA model (a) the effect of the bending angle at different air pressures, (b) the motion path of the end and middle positions of the actuator, and (c) the relationship between the bending angle and air pressure.

The deformation of the SPA is affected by the bending angle which is related to the air pressure. Fig. 6(a) show various bending angles of the basic SPA configuration at different air pressure levels. To determine the bending angle, the position of the reference point P1 is (20,0), and the point P2 and P3 in (1) can be determined. The motion path of points P2 and P3 are shown in Fig. 6(b) while compressing air into the actuator. The relationship between the air pressure and the bending angle is illustrated in Fig. 6(c), which is approximately linear when the air pressure is varied from 1 kPa to 20 kPa. This result can be used to approximate the operating pressure for the soft robot gripper according to the user requirements.

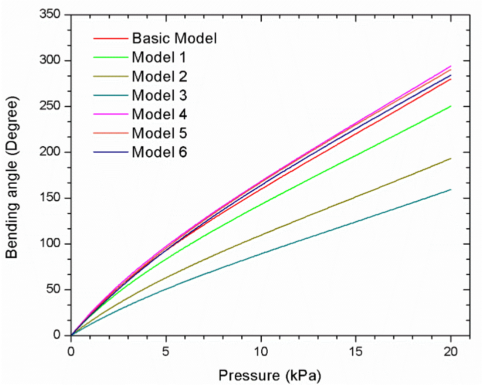

Figure 7. Bending angle and air pressure relationship.

This work simulates various SPA models, described in Section II (B), using the FEM to observe the bending angle effect. The bending angle can be influenced by the cross-section ratio of the chamber as shown in Fig. 7. Models 1, 2 and 3 have small cross-section ratios; this is accomplished by increasing the height of the models to keep air surface area in the chamber as the same for all models. The bending angle of the small cross-section ratio models (Models 1-3) have trend lines below the bending angle of the basic SPA model. This is because the air pressure acts stretching the chamber on the horizontal axis rather than the vertical axis. This increases the air flow's surface area as well as the height of the chamber. By investigating relationship between the bending angle and cross-section ratio. It is found that the bending angle reduces as cross-section ratio decreases for Models 1, 2 and 3. This effect is dominant in Model 3, which has the smallest cross-section ratio (3:1) and yields a bending angle 120 degrees lower than that of the basic model at the maximum air pressure supply.

On the other hand, Models 4, 5 and 6 have the higher cross-section ratios, which decreases the height of the chamber to maintain the air flow surface area to be the same as the basic model. The trend line of Models 4, 5 and 6 are similar to each other, the results show that the bending angle is higher than that of the basic model. The bending angle trend line of Model 4 is higher than that of Models 5 and 6 under the same pneumatic pressure. However, the gap between those trends has a minor difference. On the other hand, the models with the reduced cross-section ratios have large difference bending angle change among the three models. Therefore, the cross-section ratio has a significant impact on the bending angle. The higher the cross-section ratio, the larger the bending angle trend line. Furthermore, these simulation results provide a guide line for users to customize the SPA model suiting their applications.

V. Conclusions

This paper compares various design of the SPA models by using finite element analysis to observe the relationship between the bending angle and surface area ratio. This is helpful in the design process of the SPA and especially useful for gripper applications. The models are compared in terms of the cross-section ratio (from low to high). Each simulated model has the same material properties and boundary conditions. The simulated material is silicone rubber and the investigated conditions is under the same chamber area with the same input pressure range, which is introduced into non-linear FEM modeling program to monitor the SPA bending effect. It is found that the lower cross-section ratio resulting in significant reducing bending angle. The higher cross-section ratio has increased the bending angle. However, the higher cross-section ratio has significantly deformation effect greater than the lower cross-section ratio. Thus, if some applications need additional curvature to grasp objects, then the cross-section ratio of the actuator should be high. On the other hand, if other applications require less bending, then the cross-section ratio of the actuator should be reduced. Furthermore, the simulation results can be used to design and fabricate the soft pneumatic gripper that suit any specific application, and this will be investigated in the future work.

Conflict of Interest

The authors declare no conflict of interest.

Author Contributions

J.A. conceived and designed the experiments; N.V. and S.G. performed conceptualization; J.A. analyzed the data and wrote the paper; P.S. reviewed and edited the paper.

Acknowledgment

The authors would like to gratefully acknowledge Department of Mechanical Engineering, Prince of Songkla University to support this work.

References

[1] S. Kim, C. Laschi, and B. Trimmer, "Soft robotics: A bioinspired evolution in robotics," *Trends in Biotechnology*, vol. 31, no. 5, pp. 287–294, 2013.

[2] C. Majidi, "Soft robotics: a perspective—current trends and prospects for the future," *Soft Robotics*, vol. 1, no. 1, pp. 5–11, 2014.

[3] Y. She, C. Li, J. Cleary, and H.-J. Su, "Design and fabrication of a soft robotic hand with embedded actuators and sensors," *J. Mechanisms Robotics*, vol. 7, no. 2, pp. 021007-021007–9, May 2015.

[4] A. Villanueva, C. Smith, and S. Priya, "A biomimetic robotic jellyfish (Robojelly) actuated by shape memory alloy composite actuators," *Bioinspiration & biomimetics*, vol. 6, no. 3, p. 036004, 2011.

[5] R. K. Katzschmann, A. D. Marchese, and D. Rus, "Hydraulic autonomous soft robotic fish for 3D swimming," in *Experimental Robotics*, 2016, pp. 405–420.

[6] B. Mosadegh *et al.*, "Pneumatic networks for soft robotics that actuate rapidly," *Advanced Functional Materials*, vol. 24, no. 15, pp. 2163–2170, 2014.

[7] R. F. Shepherd *et al.*, "Multigait soft robot," *PNAS*, vol. 108, no. 51, pp. 20400–20403, Dec. 2011.

[8] J. Zhou, S. Chen, and Z. Wang, "A soft-robotic gripper with enhanced object adaptation and grasping reliability," *IEEE Robotics and Automation Letters*, vol. 2, no. 4, pp. 2287–2293, Oct. 2017.

[9] Z. Wang, Y. Torigoe, and S. Hirai, "A prestressed soft gripper: design, modeling, fabrication, and tests for food handling," *IEEE Robotics and Automation Letters*, vol. 2, no. 4, pp. 1909–1916, Oct. 2017.

[10] T. Nishimura, K. Mizushima, Y. Suzuki, T. Tsuji, and T. Watanabe, "Variable-grasping-mode underactuated soft gripper with environmental contact-based operation," *IEEE Robotics and Automation Letters*, vol. 2, no. 2, pp. 1164–1171, Apr. 2017.
[11] Z. Wang and S. Hirai, "Soft gripper dynamics using a line-segment model with an optimization-based parameter identification method," *IEEE Robotics and Automation Letters*, vol. 2, no. 2, pp. 624–631, Apr. 2017.
[12] S. Li, D. M. Vogt, D. Rus, and R. J. Wood, "Fluid-driven origami-inspired artificial muscles," *PNAS*, vol. 114, no. 50, pp. 13132–13137, Dec. 2017.
[13] K. C. Galloway *et al.*, "Soft robotic grippers for biological sampling on deep reefs," *Soft robotics*, vol. 3, no. 1, pp. 23–33, 2016.
[14] B. B. Kang, H. Lee, H. In, U. Jeong, J. Chung, and K.-J. Cho, "Development of a polymer-based tendon-driven wearable robotic hand," in *Proc. 2016 IEEE International Conference on Robotics and Automation (ICRA)*, 2016, pp. 3750–3755.
[15] W. Hu, R. Mutlu, W. Li, and G. Alici, "A structural optimisation method for a soft pneumatic actuator," *Robotics*, vol. 7, no. 2, p. 24, 2018.

Jutamanee Auysakul She received the B.E. degree in mechatronics engineering, and the M.E. degree in mechanical engineering from Prince of Songkla University, Songkhla, Thailand, in 2009 and 2012, respectively. She received the Ph.D. degree in mechanical engineering in Harbin Engineering University, Harbin, China in 2018. She has joined the Department of Mechanical Engineering, Prince of Songkla University since 2013 as a lecturer. Her current research interested include robotics and image processing.

Nitipan Vittayaphadung He received the B.Eng. degree in mechatronics engineering in Prince of Songkla University, Songkla, Thailand in 2008. He also received the M.Eng. degree in mechanical engineering in Prince of Songkla University, Songkla, Thailand in 2010. He joined the Department of Mechanical Engineering, Prince of Songkla University in 2011 as a Lecturer. He has been teaching several courses for under-graduated students such as Engineering Mechanics, Fluid Mechanics, Instrumentation, Fundamental of Mechatronics Engineering, and Mechanical Engineering Drawing. His current research interests include electrical vehicle, robotics, automation, and smart farming.

Sarawut Gonsrang He received this B.Eng. and M.Eng. in Mechanical Engineering and Materials Engineering, respectively, at Prince of Songkla University. He has served as a lecturer in Department of Mechanical Engineering at Prince of Songkla University since 2012. He has been conducting several courses for undergrad students, such as Thermodynamics, Dynamics, Fluid Dynamics, Engineering Control. He is a member of the Center of Excellence in Materials. Also, he is working with the electric vehicle research team, as well as a student formula club at the Faculty of Engineering, Prince of Songkla University. His current research interests are dynamic control of electric cars concerning energy saving, hybridized power source for extended-range electric vehicles, and metal powder production.

Pruittikorn Smithmaitrie He received his B.Eng. degree in mechanical engineering from Prince of Songkla University, Thailand, in 1996. After his graduation, he had received the Royal Thai Government Scholarship to pursue his M.S. and Ph.D. degrees in the United States. In 2000, he obtained the M.S. degree in mechanical engineering from Vanderbilt University, Nashville, TN. In 2004, he received the Ph.D. degree in mechanical engineering from University of Kentucky, Lexington, KY. He has been a faculty member of the Mechanical Engineering Department, Prince of Songkla University, since 1996 and became an Associate Professor in 2008. His research interests are the analysis and design of mechatronic systems and piezoelectric applications.